Fingerprinting a Transition-Structure Guest by a Building-Block Approach with an Incremental Series of Catalytic Hosts. Structural Requirements for Glyme and α,ω-Dimethoxyalkane Catalyses in *N*-Methylbutylaminolysis and Butylaminolysis of 4-Nitrophenyl Acetate in Chlorobenzene

John C. Hogan and Richard D. Gandour*

Department of Chemistry, Louisiana State University, Baton Rouge, Louisiana 70803-1804

Received September 4, 1991

Glymes, H-$(CH_2OCH_2)_n$-H, GLM(n), catalyze butylaminolysis of 4-nitrophenyl acetate in chlorobenzene. Values of k_{cat}/Oxy, where Oxy is the number of oxygens in the catalyst, increase with oligomer length up to triglyme, GLM(4), and then plateau. Optimal catalysis on a per oxygen basis requires a -$(CH_2OCH_2)_4$- fragment, which suggests a four-point recognition of the secondary ammonium ion of the zwitterionic tetrahedral intermediate (TI) (*J. Org. Chem.* **1991**, *56*, 2821-2826). Dissection of individual structural components and reassembly to the same structure of the complex verifies this model. The following kinetic studies of 4-nitrophenyl acetate in chlorobenzene have accomplished the task: (a) methylbutylaminolysis catalyzed by GLM(n), n = 2-4; (b) methylbutylaminolysis catalyzed by α,ω-dimethoxyalkanes, CH_3O-$(CH_2)_n$-OCH_3, DME(n), n = 2-10 and 12; and (c) butylaminolysis catalyzed by DME(n), n = 2-10 and 12. Experiment a has revealed that k_{cat}/Oxy is the same for GLM(2)-GLM(4). Optimal catalysis for breakdown of a zwitterionic TI with one ammonium proton only requires a -$(CH_2OCH_2)_2$- fragment. Experiment b has shown that k_{cat}/Oxy is largest for DME(2) with the values for the remaining DMEs 2-2.5-fold lower. A -CH_2CH_2- is the best spacer between the two oxygens. Thus, bifurcated hydrogen-bond formation between the two oxygens and the one ammonium proton enhances catalysis. Experiment c has revealed that k_{cat}/Oxy for DME(2) exceeds the remaining DMEs by 3-3.6-fold, except for DME(8) and DME(10), which have values of k_{cat}/Oxy only 1.7-fold slower. DME(8), the carba analogue of GLM(4), likely binds to the two ammonium protons individually with the two oxygens. DME(10) behaves similarly. GLM(4) catalysis of butylaminolysis identifies -$(CH_2OCH_2)_4$- as an optimal size. DME(8) catalysis confirms this size, although the two catalysts stabilize the two-proton ammonium ion differently. GLM(4) catalyzes butylaminolysis by forming two bifurcated hydrogen bonds. This suggested structure defines the size of the ammonium ion, which agrees with X-ray structural studies of polyether-ammonium complexes. Mechanistic proposals of butylaminolysis of aryl esters require such an ion. The results of this study confirm the structure of the ion in the rate-limiting step. This building-block approach is a method for "fingerprinting" ammonium ions in transition structures of ionogenic reactions.

Introduction

The same intermolecular forces that govern recognition in equilibrium host-guest chemistry govern the recognition of transition structures by many catalytic hosts. For example, some ionophoric hosts catalyze reactions that proceed through ionic intermediates.[1] An optimal ionophoric catalyst will have recognition sites that complement the ionic moiety in a transition structure. In principle, kinetic studies on a homologous series of catalytic hosts would identify the best structure for catalysis. From the size, spacing, and functionality of the optimal catalytic host, we can infer the size and functionality of the ionic part of the transition structure.

Ester aminolysis in aprotic solvents occurs with rate-limiting breakdown of a zwitterionic tetrahedral intermediate (TI) (Scheme I).[2] Glymes, H-$(CH_2OCH_2)_n$-H (GLM(n)), catalyze butylaminolysis of 4-nitrophenyl acetate in chlorobenzene more effectively than crown ethers.[3] The value of k_{cat}/Oxy, where Oxy = number of oxygens in GLM(n), increases with oligomer length up to triglyme, GLM(4), and then plateaus.[2] Optimal catalysis on a per oxygen basis requires a -$(CH_2OCH_2)_4$- fragment. Combining the zwitterionic TI for butylaminolysis with this fragment suggests the complex, shown below.

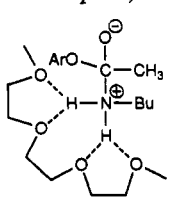

* Author to whom correspondence should be addressed.

Scheme I

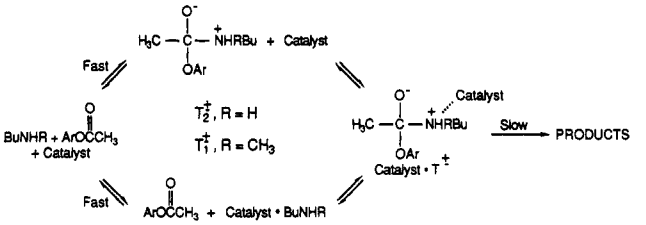

We envision a four-point recognition of the secondary (two-proton) ammonium ion.[2] We demonstrate herein the feasibility of this model by dissecting the individual structural components of the guest and the catalytic host and reassembling these components to the same structure of the complex. The following kinetic studies of 4-nitrophenyl acetate in chlorobenzene accomplish the task: (a) *N*-methylbutylaminolysis catalyzed by GLM(n); (b) *N*-methylbutylaminolysis catalyzed by α,ω-dimethoxyalkanes, CH_3O-$(CH_2)_n$-OCH_3 (DME(n)); and (c) butylaminolysis catalyzed by DME(n). Experiment a reveals the number of oxygens that are required for optimal catalysis for breakdown of a zwitterionic TI with one ammonium proton, $T_1^{\pm}$. Experiment b measures catalytic efficacy in this reaction as a function of the spacing between the oxygens. Experiment c measures the same catalytic efficacy in a reaction with two ammonium protons in the zwitterionic TI, $T_2^{\pm}$. Together with previous data, these new data effectively "fingerprint" the ammonium ion-polyether in-

(1) Cram, D. J.; Trueblood, K. N. *Top. Curr. Chem.* **1981**, *98*, 43-106.
(2) Hogan, J. C.; Gandour, R. D. *J. Org. Chem.* **1991**, *56*, 2821-2826.
(3) Hogan, J. C.; Gandour, R. D. *J. Am. Chem. Soc.* **1980**, *102*, 2865-2866.

0022-3263/92/1957-0055$03.00/0

Table I. Synthetic Parameters for Preparations of $CH_3O-(CH_2)_n-OCH_3$, n = 3–5 [DME(n)]

	DME(3)	DME(4)	DME(5)
wt, g (mequiv) of diol used	5.00 (156)	5.00 (111)	5.00 (96.0)
wt, g (mequiv) of NaH/oil used	15.0 (313)	11.0 (229)	11.0 (229)
wt, g (mequiv) of MeI used	45.0 (317)	35.0 (247)	35.0 (247)
wt, g (mequiv) of diether recovd	1.99 (43.2)	2.39 (40.1)	3.66 (55.4)
isolated yield	27.7%	36.2%	58.0%
bp, °C	105.3	131.5	159.2
lit. bp, °C	105.5[a]	132[b]	157–157.5[c]

[a] Reference 4. [b] Reference 5. [c] Reference 6.

teraction in the rate-limiting transition state. This study serves as a paradigm for elucidating the structure of an ammonium ion in a transition state of an ionogenic reaction.

Experimental Section

Materials. Chlorobenzene (Alfa/Morton Thiokol), butylamine (Aldrich), methylbutylamine (Aldrich), metallic sodium (Aldrich), iodomethane (Aldrich), 1,2-dimethoxyethane (Aldrich), 4-nitrophenyl acetate (Aldrich), toluenesulfonyl chloride (Aldrich), anhydrous methanol (Mallincrodt), reagent pyridine (Reilly), and the α,ω-alkanediols (Aldrich) were all used as received. Sodium hydride (Aldrich), obtained as a 50% dispersion in mineral oil, was treated with pentane to remove mineral oil as described below. Ethyl ether, a good commercial anhydrous reagent grade, was freshly distilled from a molten mixture of Na and K. A good commercial anhydrous reagent grade of 1,4-dioxane, was freshly distilled from molten Na. Technical grade dichloromethane (Van Waters and Rogers) was distilled from CaH.

Lower Series Diethers, DME(n), n = 3–5. (See Table I for quantities of materials used and isolated). Three samples of excess NaH oil dispersion were weighed out in three-necked reaction flasks, and each sample was washed with stirring, with pentane (5 × 25 mL). Pentane washes were decanted and discarded after stirring was discontinued and the solid material had settled. The reaction flasks were then charged with dry ether (75 mL) followed by the α,ω-diol (5.00 g) corresponding to the target diether. The resulting three-phase (one solid and two liquid phases) mixtures were stirred at reflux overnight, during which time they became two-phase (one solid and one liquid phase) mixtures. To each of the resulting reaction mixtures was added a solution of excess CH_3I in dry ether (25 mL). These mixtures were stirred at reflux for 8 h and then cooled to rt without stirring, yielding a series of three two-phase (one clear liquid and one white solid phase) mixtures. Each of the resulting liquid organic phases was decanted away from remaining solid material. The remaining solids were then washed with dry ether (2 × 50 mL). The washes were combined with the corresponding decanted liquids and filtered separately through glass frits. Fractional distillation yielded colorless oils, which were purified (≥97% pure by GC analysis) by preparative GC on a 5-ft, 15%, SE-30/Chromasorb-P (60–80-mesh) column using a GOW-MAC Model 350 gas chromatograph. ^1H FT-NMR spectra (100 MHz, $CDCl_3$) were consistent with the pure diethers. Bp's agreed with those reported previously[4-6] (see Table I).

Higher Series Diethers, DME(n), n = 6–10, 12. (See Table II for quantities of materials used and isolated.) Six Erlenmeyer flasks were each charged with pyridine (50.0 mL, 618 mequiv) and α,ω-diol (5.00 g) corresponding to a given target diether and cooled to 5 °C, after which a solution of excess TsCl in cold (5 °C) CH_2Cl_2 (100 mL) was added to each flask. The temperature of each reaction was maintained at 5–15 °C in a cold (−15 °C) ethylene glycol bath with swirling. Swirling was continued for ≈20 min, or until reaction temperatures climbed by less than 3 °C/min without the aid of the cooling bath. The resulting reaction flasks were stoppered and stored in a −10 °C freezer overnight. The contents of each flask were then poured over cracked ice (100 g). Cold (5 °C) 6 N HCl was then added to each resulting mixture, with stirring, until the aqueous layers of these mixtures turned pH paper red. Most of the ice melted in each mixture. The resulting three-phase mixtures were separated into ice/aqueous and organic components, and the ice/aqueous layers were each extracted with cold (5 °C) CH_2Cl_2 (50 mL). Corresponding CH_2Cl_2 extracts were combined with their respective organic reaction mixture components, and each of the resulting mixtures was extracted with 6 N HCl (3 × 150 mL). The resulting organic layers were each washed with water (150 mL), dried ($MgSO_4$), filtered, and concentrated (rotary evaporation using water aspirator). Residual solvents were removed overnight at reduced pressure (1 Torr) from each of the resulting off-white solids. Proton FT-NMR spectra (100 MHz, $CDCl_3$) of these solids were all consistent with pure α,ω-ditosylates corresponding to target α,ω-dimethoxyalkanes. These ditosylates were used without further analysis or purification.

To each of six 1000-mL three-necked reaction flasks were added, with swirling, CH_3OH (100 mL, 2.47 equiv) and Na (3.00 g, 10.13 equiv). Vigorous reactions ensued, which resulted in complete dissolution of the Na into clear solutions. The six ditosylates (8.00 g each) were added into these six NaOMe solutions, and stirring was initiated. After 5–10 min, the resulting reaction mixtures foamed badly for ≈1 h and then stabilized, yielding white precipitates under yellow solutions. These latter reaction mixtures were stirred at reflux overnight, cooled to rt, and partitioned between water (100 mL) and ether (100 mL). The resulting organic layers were each washed with water (3 × 100 mL), dried ($MgSO_4$), filtered, and concentrated (rotary evaporation using water aspirator), yielding six yellow oils. Bulb-to-bulb (Kugelrohr) distillation yielded clear oils, which were then purified (≥97% pure by GC analysis) by preparative GC as described above. Bp's were estimated chromatographically,[7] assuming (a) bp's of diethers are linearly related to the logs of their retention times and (b) diethers behave similarly to linear hydrocarbons under the chromatographic conditions outlined previously. Linear hydrocarbon standard mixtures (Alltech Assoc., Inc.) were used to calibrate the bp vs log retention time for the column temperatures and flow rates at which these analyses were performed. All estimated bp's agreed reasonably with those reported previously,[8-11] except for DME(6), for which no bp could be found, and DME(12), for which the two[12,13] bp's disagreed by ca. 100 °C when extrapolated to 760 Torr (see Table II). Proton FT-NMR spectra ($CDCl_3$) were consistent with pure higher series diethers.

Kinetics. Kinetic runs were performed and analyzed as before.[2] Catalytic activities (k_{cat}) for all kinetics runs were obtained from observed pseudo-first-order rate constants (k_{obs}) via the rate equation: $k_{obs} = k_0[\text{amine}]^2 + k_{cat}[\text{amine}][\text{catalyst}]$. Values of k_{cat} were obtained from the slopes of plots of $k_{obs}/[\text{amine}]$ vs [catalyst]; 301 k_{obs} values were measured in the current study (see the supplementary material).

Results

Experimental Determination of the Role of Polyether Oxygens and Ammonium Hydrogens in Catalytic Binding. To clarify the interaction between a $-(CH_2OCH_2)_4-$ segment in a catalytic host and the two ammonium hydrogens of $T_2^{\pm}$ to which it presumably binds, we studied (a) catalysis by GLM(n) of *N*-methylbutyl-

(4) Hall, R. H.; Stern, E. S. British Patent 695 789, 1953; *Chem. Abstr.* **1954**, *48*, 8816h.
(5) Meyer, F.; Krzikalla, H. German Patent 894 110, 1953; *Chem. Abstr.* **1956**, 50, 4201a.
(6) Dermer, O. C.; Hawkins, J. J. *J. Am. Chem. Soc.* **1952**, *74*, 4595–4597.
(7) Perry, J. *Introduction to Analytical Gas Chromatography: History, Principles and Practice*; Marcel Dekker: New York, 1981; Chapter 11.
(8) Dionneau, M. *Bull. Soc. Chim. Fr.* **1910**, *7*, 327–329.
(9) Meister, H. *Ber.* **1963**, *96*, 1688–1696.
(10) Braun, J. v.; Danziger, E. *Ber.* **1912**, *45*, 1970–1979.
(11) Epsztein, R. *Bull. Soc. Chim. Fr.* **1956**, 158–160.
(12) Reimschneider, R. U.S. Patent 2 973 388, 1961.
(13) Deodhar, V. B.; Dalavoy, V. S.; Nayak, U. R. *Ind. J. Chem.* **1979**, *17B*, 375–378.

Table II. Synthetic Parameters for Preparations of $CH_3O-(CH_2)_n-OCH_3$, n = 6–10, 12 [DME(n)]

	DME(6)	DME(7)	DME(8)	DME(9)	DME(10)	DME(12)
wt, g (mequiv) of diol used	5.00 (84.6)	5.00 (75.6)	5.00 (68.4)	5.00 (62.4)	5.00 (57.4)	5.00 (49.4)
wt, g (mequiv) of TsCl used	17.75 (93.08)	15.86 (83.21)	14.34 (75.23)	13.09 (68.66)	12.03 (63.10)	10.37 (54.39)
wt, g (mequiv) of ditosylate recovd	13.98 (65.56)	8.43 (38.3)	14.14 (62.20)	14.41 (61.50)	12.59 (52.50)	10.50 (41.10)
yield of ditosylate recovd	77.5%	50.6%	90.9%	98.6%	90.9%	83.3%
wt, g (mequiv) of ditosylate used	8.00 (28.1)	8.00 (36.3)	8.00 (35.2)	8.00 (34.1)	8.00 (33.2)	8.00 (31.3)
wt, g (mequiv) of diether recovd	0.97 (13)	1.52 (19.0)	2.00 (23.0)	1.76 (18.7)	2.04 (20.2)	1.25 (10.9)
single step yield	47%	52.3%	65.2%	54.8%	60.7%	34.7%
overall isolated yield	37%	26.5%	59.3%	54.0%	55.2%	28.9%
estimated bp, °C (760 Torr)	184	207	223	243	261	295
lit. bp, °C (press., Torr)	none	201[a]	108–109 (15)[b]	114–115 (10)[c]	119 (10)[d]	265–267 (760),[e] 160 (0.7)[f]

[a] Reference 8. [b] Reference 9. [c] Reference 10. [d] Reference 11. [e] Reference 12. [f] Reference 13.

aminolysis of 4-nitrophenyl acetate; (b) catalysis by DME(n) of N-methylbutylaminolysis of 4-nitrophenyl acetate; and (c) catalysis by DME(n) of butylaminolysis of 4-nitrophenyl acetate. We conducted the experiments with constant amine (~0.4 M) and ester (8.1×10^{-5} M) concentrations and a range of dilute concentrations (0.06–0.5 M) of ethers to minimize bulk solvent effects (see the supplementary material). Linear-regression analysis of k_{obs}/[amine] vs [ether] determined k_{cat}.

These experiments probe the structure of the host–guest complex by systematically varying the structure of the catalytic host and the guest. N-Methylbutylaminolysis and butylaminolysis presumably occur via a $T_1^{\pm}$ and $T_2^{\pm}$, respectively. $T_1^{\pm}$ is a one-proton analogue of $T_2^{\pm}$. 1,8-

Dimethoxyoctane (DME(8)) and 1,5-dimethoxypentane (DME(5)) model triglyme (GLM(4)) and diglyme (GLM(3)), respectively, with nonterminal oxygens replaced by methylenes. DME(2) equals GLM(2). The remaining α,ω-dimethoxyalkanes model polyethers with the nonterminal oxygens removed and with variation of the distance between the terminal oxygens.

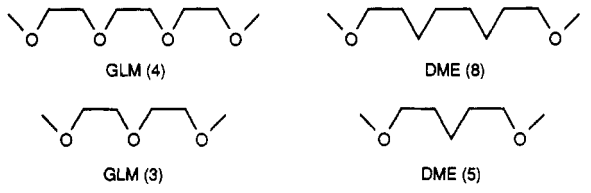

Butylaminolysis and N-Methylbutylaminolysis Catalyzed by Glymes. Data in Table III and Figure 1 profile the catalytic activities of polyethers, GLM(n), n = 2–9, in butylaminolysis and GLM(2)–GLM(4), in N-methylbutylaminolysis of 4-nitrophenyl acetate. Figure 1 plots $10^4 k_{cat}$/Oxy vs the number of oxygens in the corresponding GLM(n). The plateaus represent the maximum catalysis per oxygen for glymes—four oxygens for butylaminolysis and two oxygens for N-methylbutylaminolysis.

Butylaminolysis and N-Methylbutylaminolysis Catalyzed by α,ω-Dimethoxyalkanes. Data in Table IV and Figure 2 profile the catalytic activities of α,ω-dimethoxyalkanes, DME(n), n = 2–10 and 12, in butylaminolysis and N-methylbutylaminolysis of 4-nitrophenyl acetate. Figure 2 plots $10^4 k_{cat}$/Oxy vs the number of methylenes between the terminal oxygens of the corresponding diethers. The sharp drop in k_{cat}/Oxy from DME(2) to DME(3) followed by a slight and gradual decline to DME(12) distinguishes $-(CH_2OCH_2)_2-$ as the optimal catalytic fragment for N-methylbutylaminolysis. The value for DME(12) is the minimum. For butylaminolysis, DME(2) has a substantially larger k_{cat}/Oxy than the others, which have similar values, except for DME(8) and DME(10). Recall that DME(8) is a carba analogue of GLM(4). The value for DME(6) is the minimum, although the value is experimentally indistinguishable from those of DME(7) and DME(12).

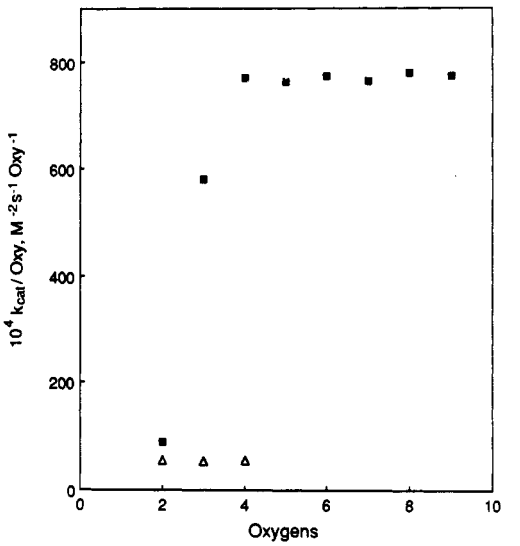

Figure 1. Plot of the per oxygen catalytic rate constant, k_{cat}/Oxy, for butylaminolysis (■) and N-methylbutylaminolysis (△) of 4-nitrophenyl acetate vs. the number of oxygens in the glyme.

Table III. Catalytic Power (k_{cat}) vs Oxygen Number Profile for Glymes Catalyzing Butylaminolysis[a] and N-Methylbutylaminolysis of 4-Nitrophenyl Acetate (8.1×10^{-5} M) in Chlorobenzene at 25 °C

		butylaminolysis		N-methylbutylaminolysis	
catalyst	oxygens	$10^4 k_{cat}$, M^{-2} s^{-1}	$10^4 k_{cat}$/Oxy, M^{-2} s^{-1} oxy^{-1}	$10^4 k_{cat}$, M^{-2} s^{-1}	$10^4 k_{cat}$/Oxy, M^{-2} s^{-1} oxy^{-1}
GLM(2)[b]	2	178 ± 3[c]	89 ± 2	111 ± 5	56 ± 3
GLM(3)	3	1740 ± 20	580 ± 7	161 ± 3	53 ± 1
GLM(4)	4	3080 ± 30	770 ± 8	220 ± 10	55 ± 3
GLM(5)	5	3810 ± 30	762 ± 6		
GLM(6)	6	4640 ± 30	773 ± 5		
GLM(7)	7	5350 ± 20	764 ± 3		
GLM(8)	8	6220 ± 80	780 ± 10		
GLM(9)	9	6970 ± 50	774 ± 6		

[a] Butylaminolysis data taken from ref 3. [b] GLM(n) = H-$(CH_2OCH_2)_n$-H. [c] Standard error.

Table IV. Catalytic Power (k_{cat}) vs Internal Methylene Number Profile for α,ω-Dimethoxyalkanes Catalyzing Butylaminolysis and N-Methylbutylaminolysis of 4-Nitrophenyl Acetate (8.1×10^{-5} M) in Chlorobenzene at 25 °C

		N-methylbutylaminolysis		butylaminolysis	
catalyst	methylenes	10^4k_{cat}, M^{-2} s^{-1}	10^4k_{cat}/Oxy, M^{-2} s^{-1} Oxy^{-1}	10^4k_{cat}, M^{-2} s^{-1}	10^4k_{cat}/Oxy, M^{-2} s^{-1} Oxy^{-1}
DME(2)[a]	2	111 ± 5	56 ± 3	178 ± 3	89 ± 2
DME(3)	3	54 ± 5	27 ± 3	62 ± 3	31 ± 2
DME(4)	4	56 ± 3	28 ± 2	68 ± 5	34 ± 3
DME(5)	5	53 ± 4	27 ± 2	67 ± 9	34 ± 5
DME(6)	6	46 ± 2	23 ± 1	50 ± 2	25 ± 1
DME(7)	7	46.2 ± 0.9	23.1 ± 0.5	57 ± 4	29 ± 2
DME(8)	8	46 ± 3	23 ± 2	108 ± 6	54 ± 3
DME(9)	9	42 ± 1	21 ± 1	69 ± 2	35 ± 1
DME(10)	10	44 ± 2	22 ± 1	105 ± 3	53 ± 2
DME(12)	12	40 ± 2	20 ± 1	53 ± 1	27 ± 1

[a] DME(n) = CH_3O-$(CH_2)_n$-OCH_3.

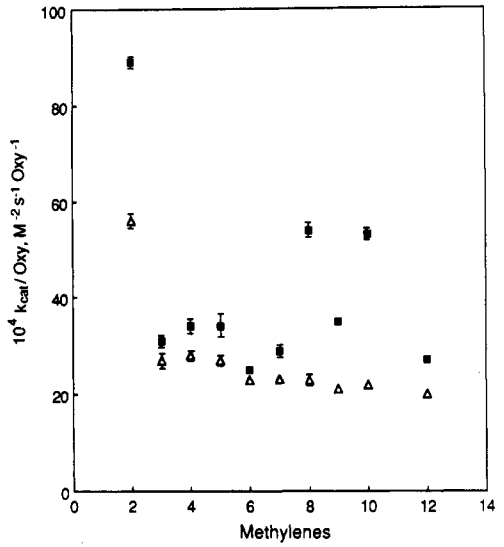

Figure 2. Plot of the per oxygen catalytic rate constant, k_{cat}/Oxy, for butylaminolysis (■) and N-methylbutylaminolysis (Δ) of 4-nitrophenyl acetate vs the number of methylene groups in α,ω-dimethoxyalkanes.

Partitioning of Catalytic Power into Individual Interactions. Cross comparisons of maximum and minimum catalyses on a per oxygen basis of the two reactions reveal the magnitude of polyether effect on transition-state stabilization (Table V). We can partition catalytic power into three interactions—one-, two-, and four-oxygen stabilization. Dividing k_{cat} by the number of oxygens normalizes catalysis to per oxygen basis. The minimum values for k_{cat}/Oxy represents one-oxygen stabilization. The minimum value for butylaminolysis is less than, but within standard error of, the k_{cat} measured[14] for tetrahydrofuran, a one-oxygen catalyst, under identical conditions. The k_{cat} values of GLM(2) represent two-oxygen stabilization, which is the maximum for catalysis of N-methylbutylaminolysis. The k_{cat} for GLM(4) in butylaminolysis represents four-oxygen stabilization, which is the maximum.

The computed transition-state stabilizations, $\Delta\Delta G^{\ddagger}$, reflect the increase in catalysis that is provided by two and four oxygens compared to one. We apply a statistical correction (number of oxygens) in computing these values. The very slight increase in one-oxygen catalysis of butylaminolysis compared to N-methylbutylaminolysis supports the strategy of methyl replacement to give a one-proton model of butylaminolysis. Two-oxygen catalysis of N-methylbutylaminolysis and butylaminolysis occur with similar enhancements compared to one-oxygen catalysis. Four-oxygen catalysis of butylaminolysis provides

(14) Su, C.-W.; Watson, J. W. *J. Am. Chem. Soc.* **1974**, *96*, 1854–1857.

Table V. Partitioning of Catalysis for Butylaminolysis and N-Methylbutylaminolysis of 4-Nitrophenyl Acetate and Associated Relative Transition-State Stabilizations

interaction	N-methylbutylaminolysis	butylaminolysis
$-CH_2OCH_2-$	20[a]	25[b]
$-(CH_2OCH_2)_2-$	111[c]	178[d]
$-(CH_2OCH_2)_4-$	N/A[e]	3080[f]
one-vs-two, $\Delta\Delta G^{\ddagger}$, kcal/mol	0.6[g]	0.8[h]
one-vs-four, $\Delta\Delta G^{\ddagger}$, kcal/mol	N/A	2.0[i]

[a] 10^4k_{cat}/Oxy, DME(12), N-methylbutylaminolysis. [b] 10^4k_{cat}/Oxy, DME(6), butylaminolysis. [c] 10^4k_{cat} GLM(2), N-methylbutylaminolysis. [d] 10^4k_{cat}/Oxy, GLM(2), butylaminolysis. [e] Not applicable. [f] 10^4k_{cat} GLM(4). [g] RT ln [111/(2 × 20)]. [h] RT ln [178/(2 × 25)]. [i] RT ln [3080/(4 × 25)].

2.0 kcal/mol more stabilization than one-oxygen catalysis. The $-(CH_2OCH_2)_2-$ and $-(CH_2OCH_2)_4-$ segments catalyze N-methylbutylaminolysis and butylaminolysis, respectively, by different interactions than one-oxygen binding.

Discussion

Bifurcated Hydrogen Bonding. The identification of $-(CH_2OCH_2)_2-$ as the optimal catalytic segment for stabilizing a one-proton ammonium ion and $-(CH_2OCH_2)_4-$ for a two-proton ammonium ion suggests that one bifurcated hydrogen bond forms in the former and that two form in the latter. X-ray crystal structures of alkylammonium ions with polyether macrocycles[1,15,16] reveal that, typically, one ammonium proton hydrogen bonds to one ether oxygen. Bifurcated hydrogen bonding occurs in cyclic[17] and acyclic[18] polyethers, but less often than one-to-one hydrogen bonding. For catalysis, bifurcation increases the effective stabilizing power of each oxygen. Using more oxygens in binding creates a tighter complex and a stronger interaction between the ammonium ion and bound oxygens.

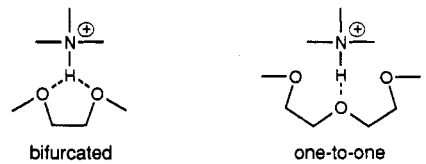

Recent molecular mechanics calculations bear on this point.[19] These calculations represent the gas phase, but

(15) Weber, E. In *Crown Ethers and Analogs*; Patai, S., Rappoport, Z., Eds.; Wiley: Chichester, 1989; Chapter 5.
(16) Goldberg, I. In *Crown Ethers and Analogs*; Patai, S., Rappoport, Z., Eds.; Wiley: Chichester, 1989; Chapter 7.
(17) Colquhoun, H. M.; Stoddart, J. F.; Williams, D. J. *J. Chem. Soc., Chem. Commun.* **1981**, 847–849.
(18) Suh, I.-H.; Saenger, W. *Angew. Chem., Int. Ed. Engl.* **1978**, *17*, 534.

apply to solvents of low polarity. Gehin et al.[19] point out that for linear hydrogen bonding in polyethers, the neighboring oxygens electrostatically stabilize the cation. One curious finding of their study is the minimum-energy structures for complexes of 18-crown-6 with primary and secondary ammonium ions. Methylammonium binds to 18-crown-6 with three linear hydrogen bonds, but dimethylammonium binds with two bifurcated hydrogen bonds. Polyethers bind ammonium ions by electrostatic forces. Whatever structure in the host that allows the greatest number of oxygens to participate will be favored. All electrostatic forces—linear hydrogen bonding, bifurcated hydrogen bonding, and Coloumbic attraction—strongly contribute to stabilization.

GLM(*n*) Catalysis of *N*-Methylbutylaminolysis. Glyme catalysis of *N*-methylbutylaminolysis occurs by formation of a bifurcated hydrogen bond to two contiguous polyether oxygens. No matter what the oligomer length, k_{cat}/Oxy remains constant. Additional oxygens only contribute on a statistical basis, e.g., k_{cat} for GLM(3) exceeds that for GLM(2) but both have identical values of k_{cat}/Oxy. GLM(3) has two sites for a bifurcated hydrogen bond to two contiguous oxygens but GLM(2) has only one. The two terminal oxygens in GLM(3) might form a bifurcated hydrogen bond, but the DME(*n*) experiments rule out this possibility.

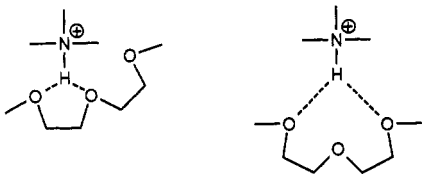

DME(*n*) Catalysis of *N*-Methylbutylaminolysis. DME(*n*) catalysis of *N*-methylbutylaminolysis reveals that two oxygens separated by two methylenes has the optimal structure for bifurcated hydrogen bonding. The k_{cat}/Oxy of DME(2) is more than 2-fold larger than those of the other DME's. DME(3)–DME(5) catalyze the reaction slightly better than the rest. DME(5), the carba analogue of GLM(3), shows no special catalytic efficacy. This lack of catalytic enhancement confirms that GLM(3) catalyzes the reaction by a bifurcated hydrogen bond that is similar to the one formed by GLM(2).

GLM(*n*) Catalysis of Butylaminolysis. Catalysis by GLM(4) and longer GLM's likely occurs by formation of two bifurcated hydrogen bonds. Perhaps the central oxygens of $-(CH_2OCH_2)_4-$ are only spacers, and the first and fourth oxygens each bind one of the two ammonium protons. The latter structure has not been seen in crystal structures of ammonium–polyether complexes. GLM(4) exhibits more catalysis than just doubling the effect of GLM(2). The four oxygens of GLM(4) must cooperate in stabilizing the ion.

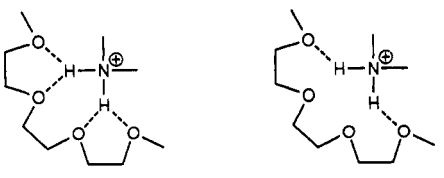

The value of k_{cat}/Oxy for GLM(3) is over six times that of GLM(2). This substantial increase suggests that GLM(3) catalyzes by binding both ammonium protons at the catalytic site. GLM(3) uses either two or three oxygens to bind the two protons. The two oxygen–two proton model resembles the typical ammonium–polyether structure observed in crystals. The central oxygen might contribute electrostatically or conformationally or both.

GLM(4) shows a 30% larger k_{cat}/Oxy than GLM(3) in butylaminolysis. GLM(4) likely binds all four oxygens to the two ammonium protons at the catalytic site and bridges these protons more effectively than GLM(3). Given the behavior of DME(8) (plotted in Figure 2), bridging is probably optimized in GLM(4). Apparently, GLM(4) catalyzes butylaminolysis by bringing together two pairs of bifurcating oxygens to form a doubly bifurcated hydrogen-bonded catalyst–substrate complex.

DME(*n*) Catalysis of Butylaminolysis. DME(*n*) catalysis of butylaminolysis shows vinculoselectivity.[20] DME(2), the best catalyst, probably forms a bifurcated hydrogen bond with one of the two ammonium protons. DME(8) and DME(10) must bind both ammonium protons because DME(8) and DME(10) do not enhance catalysis of *N*-methylbutylaminolysis. DME(8) and DME(10) bridge the two ammonium protons, presumably via one-to-one hydrogen bonds. DME(9), the diether between DME(8) and DME(10), shows no enhanced catalytic activity. Apparently, DME(9) cannot easily assume a con-

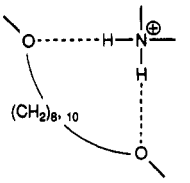

formation that is suitable for bridging the two ammonium protons in butylaminolysis. The terminal oxygens in GLM(4), DME(8), and DME(10) bridge the two ammonium hydrogens at the butylaminolysis catalytic site. The k_{cat} for GLM(4) exceeds those for DME(8) and DME(10) by 29-fold. GLM(3) shows about a 25-fold increase in k_{cat} over DME(5). The central oxygen(s) in GLM(3) and GLM(4) must be involved in binding.

Transition Structure. The combined studies indicate that the transition structure contains an ammonium ion. Kinetics studies directly report energy changes between reactants and the rate-limiting transition state. Incrementally varying the structure of a catalyst identifies the optimal host structure. Polanyi[21] has pointed out that a catalyst stabilizes the structure at the transition state. The methods described above help to size the ionic part of the transition structure. GLM(*n*) catalysis of butylaminolysis identifies $-(CH_2OCH_2)_4-$ as an optimal size. DME(*n*) catalysis confirms this size, although the two catalysts stabilize the two-proton ammonium ion differently. GLM(*n*) catalysis of *N*-methylbutylaminolysis establishes $-(CH_2OCH_2)_2-$ as the optimal segment for catalysis. DME(*n*) catalysis of this reaction supports the claim that this segment forms a bifurcated hydrogen bond to the one ammonium proton. Extrapolation of this claim to butylaminolysis suggests two bifurcated hydrogen bonds in the $T_2^{\pm}$·$-(CH_2OCH_2)_4-$ complex.

(19) Gehin, D.; Kollman, P. A.; Wipff, G. *J. Am. Chem. Soc.* **1989**, *111*, 3011–3023.

(20) Morton, T. H.; Beauchamp, J. L. *J. Am. Chem. Soc.* **1975**, *97*, 2355–2362.

(21) Polyani, M. *Z. Electrochem.* **1921**, *27*, 142–150.

This hypothesized structure defines the size of the ammonium ion. X-ray (equilibrium) structural studies of polyether–ammonium ion complexes suggest that $-(CH_2OCH_2)_4-$ is the optimal size for a polyether binding of a two-proton ammonium ion. The mechanism of butylaminolysis of aryl esters requires such an ion.[3,14,22] This study has confirmed this ionic structure in the rate-limiting step and demonstrated the combined use of kinetics and host–guest structural methods to size an ion in a transition structure. We offer this building-block approach as a general method for sizing ammonium ions in ionogenic reactions. An ionophoric catalyst, however, will only influence the course of an ionogenic reaction and the claims only apply to that reaction.

Mechanism of Catalysis. 1. Transition-Structure Stabilization. Comparisons of the transition-state stabilizations (Table V) with the proposed host–guest structures reveal the relative energies of the different hydrogen-bonding interactions. One-oxygen catalysis represents a single one-to-one hydrogen bond. The slight increase in one-oxygen catalysis for butylaminolysis compared to that for *N*-methylbutylaminolysis may reflect the slightly less stable ammonium ion in the former. In the gas phase, the difference in stabilization by GLM(2) versus dimethyl ether decreases for a tertiary ammonium ion compared to a primary ammonium ion.[23] Catalysis (stabilization) occurs where most needed.[24] Two-oxygen catalysis for *N*-methylbutylaminolysis represents stabilization by bifurcated hydrogen bonding to one proton, 0.6 kcal/mol. Comparing k_{cat} for GLM(2) and one-oxygen catalysis of butylaminolysis gives 0.8 kcal/mol. The above suggestion of a less stable ammonium ion in butylaminolysis also explains the slight increase in stabilization by a single bifurcated hydrogen bond. This internal consistency in stabilization establishes the catalytic enhancement of bifurcated over one-to-one hydrogen bonding.

Stabilization by GLM(4) in butylaminolysis involves cooperativity or proximity effects or both. The individual effects are small, but when combined produce significant catalysis. The point, however, is to show how to deduce the structure of a four-oxygen catalyst from the dissection of the individual contributions to catalytic power. GLM(4) stabilizes the butylaminolysis transition structure by 2.0 kcal/mol, which exceeds the expected contribution ($0.8 \times 2 = 1.6$) for two (unconnected) bifurcated hydrogen bonds by 0.4 kcal/mol. The catalytic enhancement for DME(8) and DME(10) over minimal catalysis measures the contribution (0.4 kcal/mol) from proximity for two concurrent one-to-one hydrogen bonds with the correct spacing of acceptors. The agreement in the two comparisons may be a valid measure of the proximity effect or just coincidence. GLM(4) catalyzes by using two concurrent bifurcated hydrogens, so the proximity contribution might be different. Certainly, the population of molecules in conformations suitable for catalysis increases in going from DME(8) to GLM(4), because of the more favorable gauche interaction in a $-OCH_2CH_2O-$ segment.[25] This conformational difference complicates comparisons between the two catalysts.

2. Rate-Limiting Step. Scheme II summarizes the possible paths from $T^{\pm}$ to products. $T^{\pm}$ must lose one ammonium hydrogen and the aryl oxide nucleofuge. Aryl

Scheme II

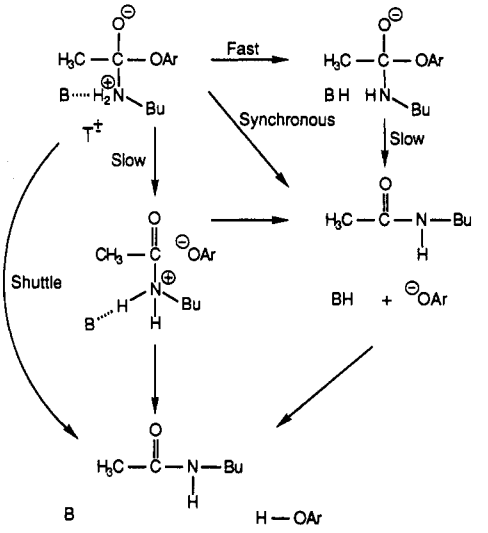

oxide expulsion from $T^{\pm}$ limits the rate in glyme-catalyzed butylaminolysis of aryl acetates in chlorobenzene.[2] Four paths are possible: (a) a fast proton transfer from $T^{\pm}$ to B, followed by slow aryl oxide expulsion; (b) slow aryl oxide expulsion to form N-protonated amide followed by rapid proton transfer to B or aryl oxide; (c) proton transfer to B synchronous with aryl oxide expulsion; and (d) proton shuttle to aryl oxide during expulsion.

a. Proton Transfer, Then Slow Aryl Oxide Expulsion. If proton loss from $T^{\pm}$ precedes aryl oxide expulsion, then the proton transfer will limit the rate because the subsequent aryl oxide expulsion is energetically favorable. Base catalysts strong enough to deprotonate $T^{\pm}$ in aprotic media, e.g., tetrahexylammonium benzoate,[26] change the rate-determining step from decomposition to formation of $T^{\pm}$. This rate-determining step change is impossible, if deprotonation of $T^{\pm}$ is fast. Proton transfer must limit the rate or occur after aryl oxide expulsion. Results of previous experiments[2,14] support the latter.

b. Aryl Oxide Expulsion, Then Proton Transfer. If aryl oxide expulsion from $T^{\pm}$ precedes proton transfer, then hydrogen bonding by base catalysts to the ammonium hydrogens should stabilize the rate-determining transition structure. Su and Watson[14] have observed that catalysis correlates with hydrogen-bonding ability and not base strength. Hydrogen bonding should also stabilize the N-protonated amide[27] intermediate, which otherwise would be unstable in nonpolar media. Furthermore, an N-protonated amide would be a tight ion pair in nonpolar media.

If proton abstraction by ethers occurs during the rate-determining step, then the catalytic activities of ether catalysts in aminolysis should parallel the proton stabilization energies of the same set of ethers in a nonpolar medium, such as the gas phase. Sharma et al.[28] have shown that the gas-phase proton is stabilized somewhat less by GLM(3) than by DME(5). In nonpolar aminolysis, GLM(3) is a much better catalyst than DME(5). We conclude that ether catalysts do not abstract protons in the rate-determining step of ester aminolysis in chlorobenzene. The rate-determining step in ester aminolysis occurs after ether catalysts bind to the ammonium ion. When ethers or other

(22) Nagy, O. B.; Reuliaux, V.; Bertrand, N.; Van Der Mensbrugghe, A.; Leseul, J.; Nagy, J. B. *Bull. Soc. Chim. Belg.* **1985**, *94*, 1055–1074.
(23) Meot-Ner (Mautner), M. *J. Am. Chem. Soc.* **1983**, *105*, 4912–4915.
(24) Jencks, W. P. *Chem. Rev.* **1972**, *72*, 705–718.
(25) Baldwin, D. T.; Mattice, W. L.; Gandour, R. D. *J. Comput. Chem.* **1984**, *5*, 241–247.
(26) Menger, F. M.; Vitale, A. C. *J. Am. Chem. Soc.* **1973**, *95*, 4931–4934.
(27) Perrin, C. L. *Acc. Chem. Res.* **1989**, *22*, 268–275.
(28) Sharma, R. B.; Blades, A. T.; Kebarle, P. *J. Am. Chem. Soc.* **1984**, *106*, 510–516.

bases (aryl oxide or butylamine) abstract protons, it occurs after the rate-determining step.

c. Synchronous Proton Transfer and Aryl Oxide Expulsion. Coupling proton transfer with aryl oxide expulsion avoids formation of the N-protonated amide. Such a transition structure should have a similar or slightly smaller ammonium ion fragment than a hydrogen-bonded complex. This mechanism should correlate catalysis with basicity more than with the hydrogen-bonding ability of a catalyst. In light of Su and Watson's data,[14] we discount this mechanism.

d. Proton Shuttle to Aryl Oxide. One can imagine a concerted pathway where the proton is transferred to the departing aryl oxide. Such a mechanism agrees with the Hammett study[3] and the hydrogen-bonding study,[14] but this mechanism requires the coupling of many motions.

3. Conclusion. We favor mechanism b with aryl oxide as the proton acceptor. Ether or butylamine may do the actual abstraction, provided that this activity occurs in a fast step after the rate-determining step. Does the proton transfer to aryl oxide occur in a separate step? We cannot imagine how aryl oxide accepts the proton without disrupting the strong hydrogen bonding between polyether and N-protonated amide. The tight ion pair must be an intermediate, with proton loss easier than reformation of a TI. The aryl oxide nucleofuge may either take a proton from an intermediary base to form the final phenol product, or it may abstract a proton directly from the N-protonated amide polyether complex (or a less complexed form).

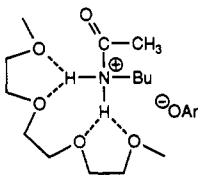

Summary

Glyme-catalyzed ester aminolysis in chlorobenzene shows transition-structure recognition in which a catalyst binds an ionic group that is attached to the site of reaction. *The number of ammonium protons in the transition structure determines both the number of polyether oxygens needed for optimal catalysis and the optimal spacing among these oxygens.* We have "fingerprinted" this ammonium ion by systematically varying the structure of ionophore catalysts and the number of protons in the ammonium ion of the transition structure. We offer the methods described above as paradigm for determining transition structure in aminolysis reactions.

Acknowledgment. We thank Mr. Don Patterson for technical assistance. We dearly thank Mrs. Mary Jane Peters for her encouragement.

Registry No. DME(3), 17081-21-9; DME(4), 13179-96-9; DME(5), 111-89-7; DME(6), 13179-98-1; DME(7), 137333-33-6; DME(8), 51306-09-3; DME(9), 91337-21-2; DME(10), 53759-62-9; DME(12), 73120-52-2; GLM(2), 110-71-4; GLM(3), 111-96-6; GLM(4), 112-49-2; GLM(5), 143-24-8; GLM(6), 1191-87-3; GLM(7), 1072-40-8; GLM(8), 1191-91-9; GLM(9), 25990-94-7; 1,3-propanediol, 504-63-2; 1,4-butanediol, 110-63-4; 1,5-pentanediol, 111-29-5; 1,6-hexanediol, 629-11-8; 1,7-heptanediol, 629-30-1; 1,8-octanediol, 629-41-4; 1,9-nonanediol, 3937-56-2; 1,10-decanediol, 112-47-0; 1,12-dodecanediol, 5675-51-4; 1,6-hexanediol ditosylate, 4672-50-8; 1,7-heptanediol ditosylate, 40235-95-8; 1,8-octanediol ditosylate, 36247-32-2; 1,9-nonanediol ditosylate, 73992-42-4; 1,10-decanediol ditosylate, 36247-33-3; 1,12-dodecanediol ditosylate, 36247-34-4; 4-nitrophenyl acetate, 830-03-5; butylamine, 109-73-9; methylbutylamine, 110-68-9.

Supplementary Material Available: Observed rate constants for polyether- and diether-catalyzed aminolysis of 4-nitrophenyl acetate at 25 °C in chlorobenzene (22 pages). Ordering information is given on any current masthead page.

Synthesis of Trioxatricornan and Derivatives. Useful Keystones for the Construction of Rigid Molecular Cavities

Michael Lofthagen, Russell VernonClark, Kim K. Baldridge,† and Jay S. Siegel*

Department of Chemistry, University of California, San Diego, La Jolla, California 92093, and San Diego Supercomputer Center, 10100 John Hopkins Ave., La Jolla, California 92137

Received August 13, 1991

The synthesis of a new class of organic keystones for the development of macrocage structures is presented. These represent some of the most versatile building blocks for macrocage construction. The keystone structure developed herein can be interpreted as either a centrally alkylated [*cd,mn*]dibenzopyrene or a tris ortho-bridged triphenylmethane. We call this basic skeleton tricornan. Routes into both chiral (C_3 and C_1 symmetry) and achiral (C_{3v} symmetry) derivatives are reported. The synthesis of derivatives of the trioxatricornan keystone, leading to two macrocage structures, is presented. The X-ray structures of *cent*-methyltrioxatricornan **7** and 2,6,10-tris(dimethylamino)-*cent*-methyltrioxatricornan (**20**) are discussed and compared to that of 1,1,1-triphenylethane. Empirical force field and AM1 calculations are compared to the X-ray structures and discussed. A general discussion on the keystone analogy is presented.

The idea of a molecular keystone, developed by Whitlock[1] and applied elegantly by Diederich[2] and Dougherty[3] to the molecular construction of binding sites for organic guest molecules, stems from the architectural design of a portal or archway.[4] The molecular keystone serves a versatile role; existing both as a structural basis for mo-

† San Diego Supercomputer Center.

(1) (a) Sheridan, R. E.; Whitlock, H. W., Jr. *J. Am. Chem. Soc.* **1986**, *108*, 7120. (b) Miller, S. P.; Whitlock, H. W., Jr. *J. Am. Chem. Soc.* **1984**, *106*, 1492. (c) Jarvi, E. T.; Whitlock, H. W., Jr. *J. Am. Chem. Soc.* **1982**, *104*, 7196.

0022-3263/92/1957-0061$03.00/0